ISSN No: 2348-4845
International Journal & Magazine of Engineering, Technology, Management and Research
A Peer Reviewed Open Access International Journal

Modeling Implementation and Comparison of Wind Turbine System Using Induction Generator

K. Prakash
M.Tech Student
P.V.K.K. Institute of Technology.

V. N. Vinay Kumar
Assistant Professor
P.V.K.K. Institute of Technology.

Abstract

This paper describes the performance comparison of a wind power systems based on two different induction generators as well as the experimental demonstration of a wind turbine simulator for the maximum power extraction. The two induction machines studied for the comparison are the squirrel-cage induction generator (SCIG) and the doubly fed induction generator (DFIG). The techniques of direct grid integration, independent power control, and the droop phenomenon of distribution line are studied and compared between the SCIG and DFIG systems. Both systems are modeled in Matlab/Simulink environment, and the operation is tested for the wind turbine maximum power extraction algorithm results. Based on the simulated wind turbine parameters, a commercial induction motor drive was programmed to emulate the wind turbine and is coupled to the experimental generator systems. The turbine experimental results matched well with the theoretical turbine operation.

Index Terms: ***Doubly fed induction machines, field-oriented control, maximum power tracking, and wind power system.***

INTRODUCTION

The increasing emphasis on renewable wind energy has given rise to augmented attention on more reliable and advantageous electrical generator systems. Induction generator systems have been widely used and studied in wind power system because of their advantages over synchronous generators, such as smaller size, lower cost, and lower requirement of maintenance. The straightforward power conversion technique using squirrel-cage induction generator (SCIG) is widely accepted in fixed-speed applications with less emphasis on the high efficiency and control of power flow. However, such direct connection with grid would allow the speed to vary in a very narrow range and thus limit the wind turbine utilization and power output. Another major problem with SCIG power system is the source of reactive power; that is, an external reactive power compensator is required to hold the distribution line voltage and prevent the whole system from overload. On the other hand, the doubly fed induction generator (DFIG) with variable-speed ability has higher energy capture efficiency and improved power quality and thus has attracted more attentions.

With the advent of power electronic techniques, a back-to-back converter, which consists of two bidirectional converters and a dc link, acts as an optimal operation tracking interface between generator and grid. Field-oriented control (FOC) is applied to both rotor- and stator-side converters to achieve desirable control on voltage and power. Generally, the FOC has been presented based on DFIG mathematical equations only. However, a three-phase choke is commonly used to couple the stator-side converter into the grid. Therefore, this paper proposes the FOC schemes of stator-side converter involving the choke, and it turns out that both stator- and rotor side converter voltages consist of a current regulation part and a cross-coupling part.

First, this paper presents an experimental setup to emulate the wind turbine operation in torque control mode and thus to obtain a power operation curve for optimal power control. Second, the modeling and simulation of SCIG and DFIG wind systems are

ISSN No: 2348-4845
International Journal & Magazine of Engineering, Technology, Management and Research
A Peer Reviewed Open Access International Journal

studied. Comparison between SCIG without static var compensator (STATCOM) and SCIG with STATCOM as well as DFIG system clearly indicates difference in resulted distribution line voltage.

WIND TURBINE

Wind energy is extracted through wind turbine blades and then transferred by the gearbox and rotor hub to the mechanical energy in the shaft, which drives the generator to convert the mechanical energy to electrical energy. The turbine model is based on the output power characteristics, expressed as

$$P_m = C_p(\lambda, \beta) \cdot \frac{1}{2}\rho A v_w^3 \quad \text{(1a)}$$

$$\lambda = \frac{R_{\text{blade}}\omega_r}{v_w} \quad \text{(1b)}$$

where *Pm* is the mechanical output power in watts, which depends on power performance coefficient *Cp*, air density *ρ*, turbine swept area *A*, and wind speed *vw*. (1/2) · *ρAv*3*w* is equal.

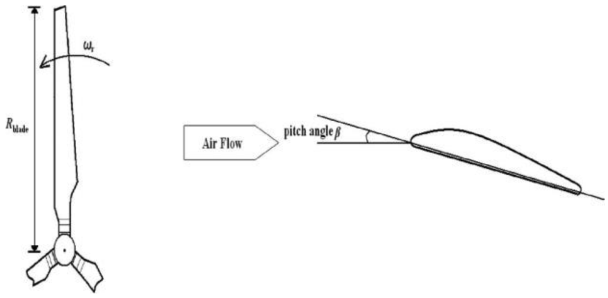

Fig. 2.4 Schematics of turbine blade from different views.

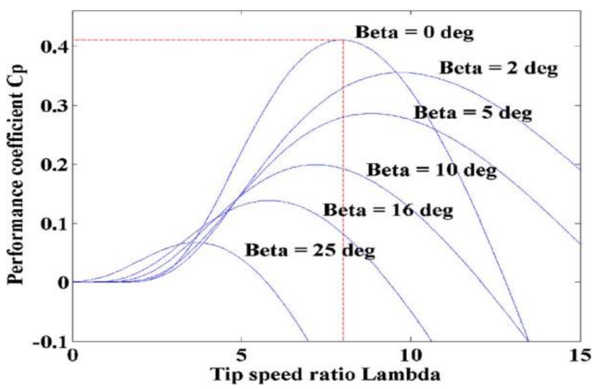

Fig. 2.5 *Cp−λ* curve for the turbine model.

To the kinetic energy contained in the wind at a particular speed *vw*. The performance coefficient *Cp*(*λ*, *β*), which depends on tip speed ratio *λ* and blade pitch angle *β*, determines how much of the wind kinetic energy can be captured by the wind turbine system. A nonlinear model describes *Cp*(*λ*, *β*) as [8]

$$C_p(\lambda, \beta) = c_1(c_2 - c_3\beta - c_4\beta^2 - c_5)e^{-c_6} \quad (2)$$

Where *c*1 = 0.5, *c*2 = 116/*λi*, *c*3 = 0.4, *c*4 = 0, *c*5 = 5, *c*6 =21/*λi*, and

$$\frac{1}{\lambda_i} = \frac{1}{\lambda + 0.08\beta} - \frac{0.035}{\beta^3 + 1} \quad (3)$$

where *R*blade and *ωr* are the blade radius and angular frequency of rotational turbine as depicted in Fig. 1. The *Cp−λ* curve for this particular turbine model at different *β* is shown in Fig. 2 where it is illustrated that, to achieve maximum *Cp*, one has *β* = 0◦ and *λ* = 8. The blade with fixed geometry will have fixed *Cp−λ* characteristics, as described in (2) and (3). Therefore, to track the optimal output power, the curve of *Pm−ωr* is the "map" to follow.

In order to experimentally investigate the operation of wind turbine, a wind turbine emulator system is built to operate in torque control mode, using (1a)

$$T = \frac{P}{\omega_r} = \frac{1}{2}\rho\pi R_{\text{blade}}^3 v_w^2 \frac{C_p}{\lambda} = \frac{1}{2}\rho\pi R_{\text{blade}}^3 v_w^2 C_m \quad (4)$$

where *Cm* is the torque performance coefficient. It is dependent on *ωr*, *vw*, and *β*. Thus, based on turbine *Cp−λ* model and Fig. 3. *Cm−λ* curve for the turbine emulator.

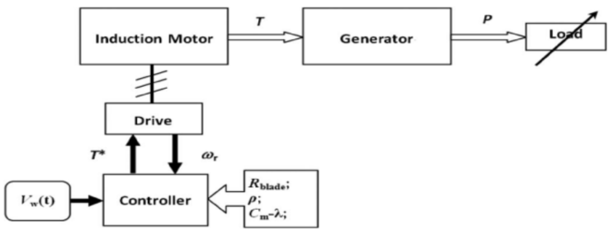

Fig 2.5 Wind turbine emulator system.

ISSN No: 2348-4845
International Journal & Magazine of Engineering, Technology, Management and Research
A Peer Reviewed Open Access International Journal

by assuming $\beta = 0^\circ$, the $Cm-\lambda$ curve is given in Fig. 3. At any particular *vw*, one could obtain different torque and, thus, power output by varying rotor speed.

SCIG WIND POWER SYSTEM

The SCIG system including the wind turbine, pitch control, and reactive power compensator. The entire system includes three stages for delivering the energy from wind turbine to the power grid. The first one is wind farm stage which handles with low voltage *V*wt, the second is distribution stage which has medium voltage *V*dis, and the third is grid transmission stage which has high voltage *V*grid.

The three-phase transformers take care of the interface between stages As mentioned, nominal power *P*nSCIG is considered as active power reference to regulate the pitch angle while *V*dis and *I*dis denote the distribution line-to-line voltage and phase current, and they are monitored to favor the reactive power compensation for distribution line. This fairly straightforward technique was first used since it is simple and has rugged construction, reliable operation, and low cost. However, the fixed-speed essential and potential voltage instability problems severely limit the operations of wind turbine.

Since SCIG is of fixed-speed generator, for a particular wind speed, the output active power is fixed as well. Thus, with the increase of wind speed, so does the output power until the nominal power is reached. The wind speed at this moment

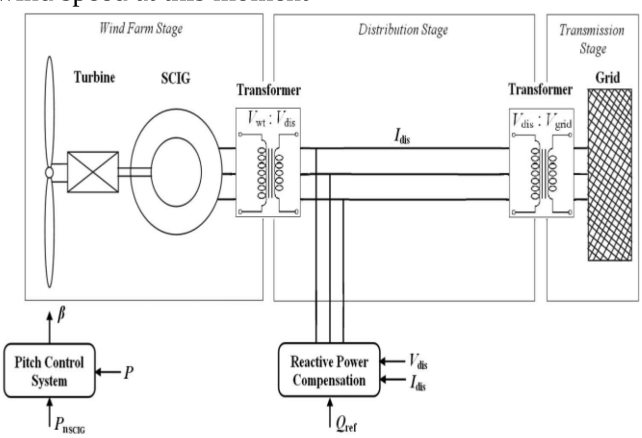

Fig. 3.1. SCIG wind power system topology.

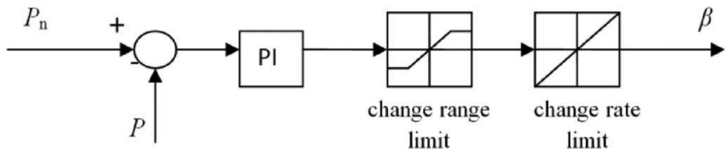

Fig. 3.2. Pitch angle control.

is called nominal wind speed. Beyond this speed, the pitch angle system will prevent the output power from exceeding the nominal value. That is, when the wind speed is below nominal value, the power capture can vary with the change of wind speed; and when the wind speed is above nominal value, the pitch angle control system will limit the generated power by changing the pitch angle. In such way, the output power will be stabilized at nominal value where the wind speed is always above nominal speed. The pitch angle is determined by an open loop control of regulated output active power and by that shown in Fig. 6. Due to the huge size of blade and, thus, inertia, pitch angle has to change in a slow rate and a reasonable range. It is also worthy to notice that, without reactive power source, in Section V, the SCIG system tends to lead to a voltage droop in distribution line which will cause overload problem. In the simulation section, the comparison between SCIG system with and without STATCOM is conducted.

DFIG WIND POWER SYSTEM

Traditionally, the dynamic slip control is employed to fulfill the variable-speed operation in wind turbine system, in which the rotor windings are connected to variable resistor and control the slip by the varied resistance. This type of system can achieve limited variations of generator speed, but external reactive power source is still necessary. Consequently, to completely remove the reactive power compensation and to control both active and reactive power independently, DFIG wind power system is one of most popular methods in wind energy applications. This paper reproduces DFIG model first of all and then concentrates on the controlling schemes of power converters, in which the active and reactive power are controlled independently. In particular, the stator-side

ISSN No: 2348-4845
International Journal & Magazine of Engineering, Technology, Management and Research
A Peer Reviewed Open Access International Journal

converter control involving an RL series choke is proposed.

Both controlling of rotor- and stator-side converter voltages end up with a current regulation part and a cross-coupling part. The wind turbine driving DFIG wind power system consists of a wound-rotor induction generator and an ac/dc/ac insulated gate bipolar transistor (IGBT)-based pulse width-modulated (PWM) converter (back-to-back converter with capacitor dc link), as shown in Fig. In this configuration, the back-to-back converter consists of two parts: the stator-/grid-side converter and the rotor-side converter. Both are voltage source converters using IGBTs, while a capacitor between two converters acts as a dc voltage source. The generator stator windings are connected directly to grid (with fixed voltage and frequency of grid) while the rotor winding is fed by rotor-side converter through slip rings and brushes, at variable frequency.

The control system is divided into two parts—stator-side converter control system and rotor-side converter control system. An equivalent circuit of DFIG is depicted in fig and the relation equations for voltage V, current I, flux Ψ, and torque Te involve are:

$$V_{ds} = R_s I_{ds} - \omega_s \Psi_{qs} + \frac{d\Psi_{ds}}{dt}$$
$$V_{qs} = R_s I_{qs} + \omega_s \Psi_{ds} + \frac{d\Psi_{qs}}{dt} \quad (5)$$

$$V_{dr} = R_r I_{dr} - s\omega_s \Psi_{qr} + \frac{d\Psi_{dr}}{dt}$$
$$V_{qr} = R_r I_{qr} + s\omega_s \Psi_{dr} + \frac{d\Psi_{qr}}{dt} \quad (6)$$

$$\Psi_{ds} = L_s I_{ds} + L_m I_{dr}$$
$$\Psi_{qs} = L_s I_{qs} + L_m I_{qr} \quad (7)$$

$$\Psi_{dr} = L_r I_{dr} + L_m I_{ds}$$
$$\Psi_{qr} = L_r I_{qr} + L_m I_{qs} \quad (8)$$

$$T_e = \frac{3}{2} n_p (\Psi_{ds} I_{qs} - \Psi_{qs} I_{ds}) \quad (9)$$

mutual inductance, the number of pole pairs, and the inertia coefficient, respectively.

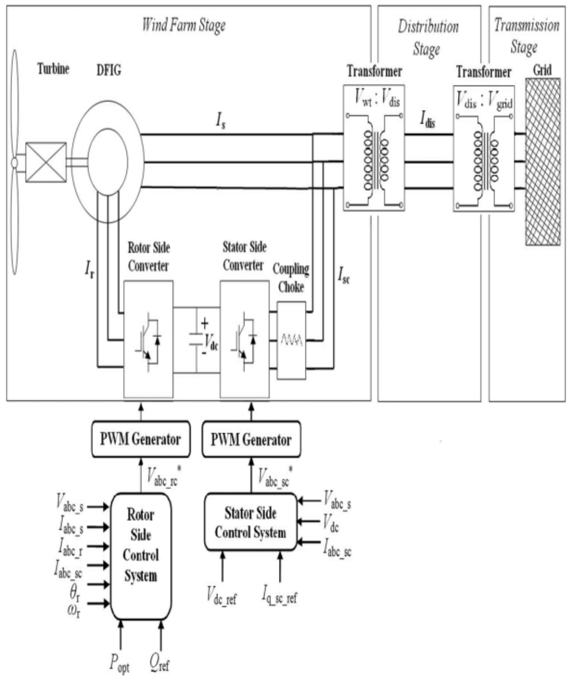

Fig. 4.1 Wind turbine–doubly fed induction generator system configuration.

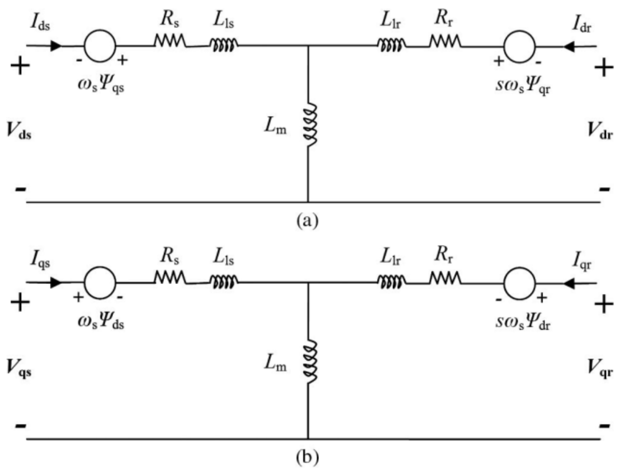

Fig. 4.2. Equivalent circuit of DFIG. (a) d-axis model. (b) q-axis model.

ISSN No: 2348-4845
International Journal & Magazine of Engineering, Technology, Management and Research
A Peer Reviewed Open Access International Journal

A. Rotor-Side Converter Control

If the derivative parts in (5) are neglected, one can obtain stator flux as

$$\Psi_{ds} = (V_{qs} - R_s I_{qs})/\omega_s$$

$$\Psi_{qs} = (V_{ds} - R_s I_{ds})/(-\omega_s)$$

$$\Psi_s = \sqrt{\Psi_{ds}^2 + \Psi_{qs}^2} \qquad (10)$$

Because of being directly connected to the grid, the stator voltage shares constant magnitude and frequency of the grid. One could make the d-axis align with stator voltage vector; it is true that Vs = Vds and Vqs = 0, thus Ψs = Ψqs and Ψds = 0, which is of stator-voltage-oriented vector control scheme, as

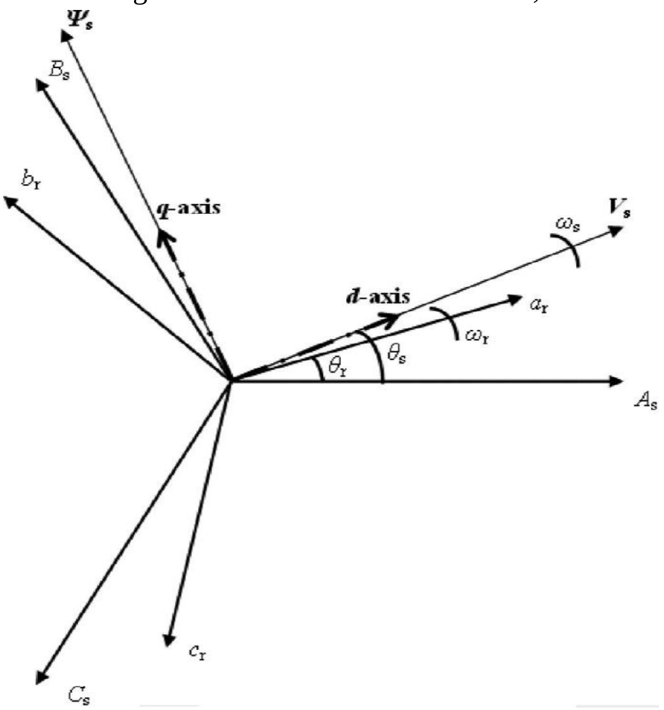

Fig. 4.3. Stator voltage FOC reference frame.

Depicted in Fig. According to the rotor-side converter reference current is derived as

$$I_{dr\_ref} = -\frac{2L_s T_e}{3n_p L_m \Psi_s} \qquad (11)$$

where

$$P_{e\_ref} = P_{opt} - P_{loss} = T_e \omega_r$$

$$P_{loss} = R_s I_s^2 + R_r I_r^2 + R_c I_{sc}^2 + F\omega_r^2 \qquad (12)$$

where Isc, Rc, and F are stator-side converter current, choke resistance, and friction factor, respectively. Popt, Pe_ref , and

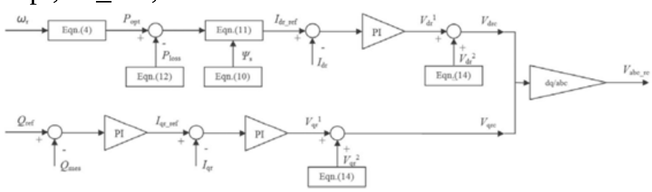

Fig. 4.4. Rotor-side converter control scheme.

Ploss are desired optimal output active power, reference active power, and system power loss. Combining the active power is used as command inputs to determine current reference Idr_ref. Meanwhile, the output reactive power is the stator reactive output power since the stator-side converter's reactive power is set to be zero. Then, one has
Qo =Qs + Qsc = Qs = Im[(Vds + jVqs)(Ids + jIqs)*] = −VdsIqs = −Vds 1/Ls (Ψs − LmIqr). (13)

Thus, the regulation of reactive power can lead to Iqr_ref , and then, the rotor-side converter voltage signals V 1 dr and V 1 qr are derived by the regulation of currents. In addition, the feed forward coupling parts V 2 dr and V 2 qr are derived based on (6) and (8), as

V 2 dr =RrIdr − sωs(LrIqr + LmIqs) V 2 qr =RrIqr + sωs(LrIdr + LmIds) (14)

where the superscripts 1 and 2 denote the current regulation part and cross-coupling part, respectively. At last, rotor-side converter voltage signals in dq-axes are expressed as

Vdrc =Vdr = V 1dr + V 2dr Vqrc =Vqr = V 1qr + V 2qr (15)

ISSN No: 2348-4845
International Journal & Magazine of Engineering, Technology, Management and Research
A Peer Reviewed Open Access International Journal

where subscript rc denotes the rotor-side converter. After the conversion of dq − abc, the rotor-side converter voltage Vabc_rc can be obtained. Fig. 10 exhibits the control scheme for the aforementioned procedure.

B. Stator-Side Converter Control

Concerning the use of three-phase series RL choke between stator- and stator-side converter, a cross-coupling model is required to derive the voltage signal of stator-side converter, as described in Fig. 11

$V_{dsc} = V_{ds} - V_{dch}$ $V_{qsc} = V_{qs} - V_{qch}$ (16)

where the subscripts sc and ch denote the variables of stator side converter and choke. The coupling part of voltage signals V_{2dch} and V_{2qch} is expressed as

$V_{2dch} = R_c I_{dsc} - \omega_s L_c I_{qsc}$ $V_{2qch} = R_c I_{qsc} + \omega_s L_c I_{dsc}$. (17)

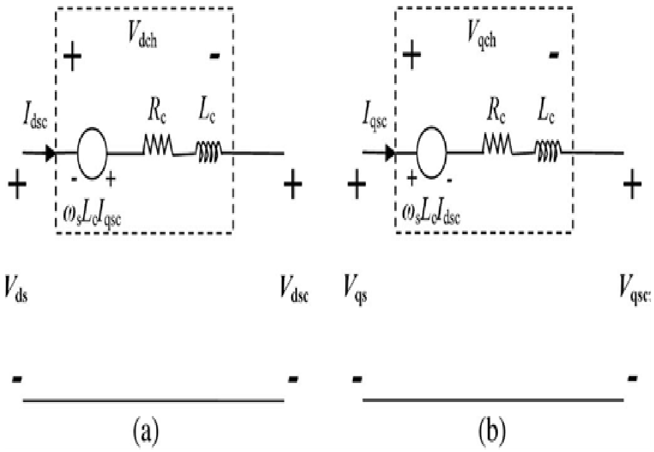

Fig. 4.5. Equivalent circuit of stator-side-converter choke. (a) d-axis model. (b) q-axis model.

Moreover, V_{1dch} and V_{1qch} are determined by the regulation of currents Idsc and Iqsc in which the current reference Iqsc_ref is given directly while Idsc_ref is determined by the regulation of dc-link voltage Vdc. Thus, above all, the stator-side converter voltage signals Vdsc and Vqsc are obtained as follows and depicted in Fig. 12:

$V_{dsc} = V_{ds} - V_{1dch} - V_{2dch}$ $V_{qsc} = V_{qs} - V_{1qch} - V_{2qch}$. (18)

SIMULATION RESULTS

In this project simulation and its results of comparison between squirrel cage induction generator system and doubly fed induction generator system as shown in below description. It has two stages.

1. Squirrel cage induction generation system with constant speed operation.
2. Doubly fed induction generator system with variable speed operation.

a. Squirrel cage induction generation system with constant speed operation

In this case, constant speed operation is possible by varying a wind speed in a narrow range that is 8 to 11 m/s. The simulation model for this case is as shown in figure 6.1

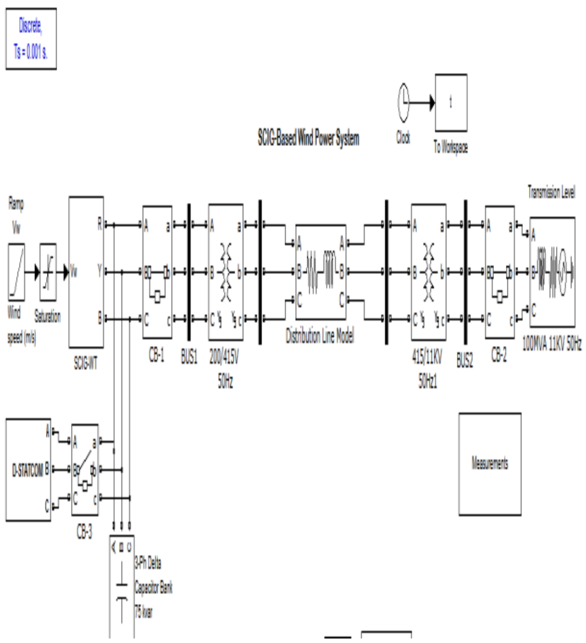

Fig 6.1 Squirrel cage induction generation system with constant speed operation

In initial method of operation ramp wind speed is given to the wind turbine that varies from t=5 to t=10 sec and it remain constant at the end of the simulation. Dynamics variations and steady state of pitch angle, generator speed, produced active power and consumed reactive power as shown below.

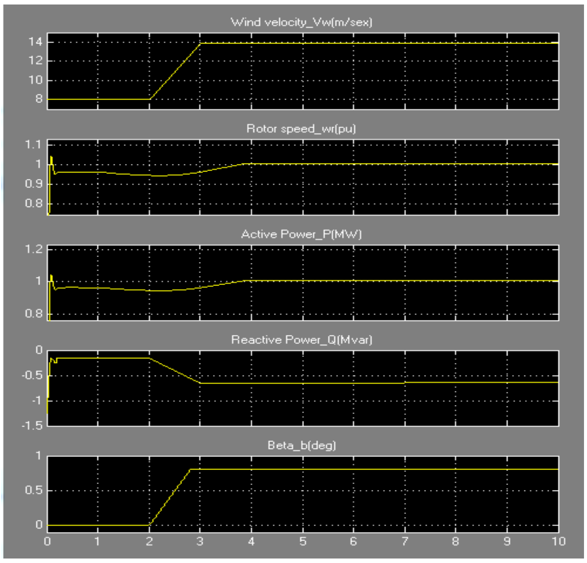

Fig 6.2 Simulation results for SCIG system.

The below waveforms shows that variations of reactive power in squirrel cage wind power system by using with and without STATCOM by connecting static var compensator the reactive power is improved at the steady state it remains produced unity power factor to improve the system performance of squirrel cage wind power system.

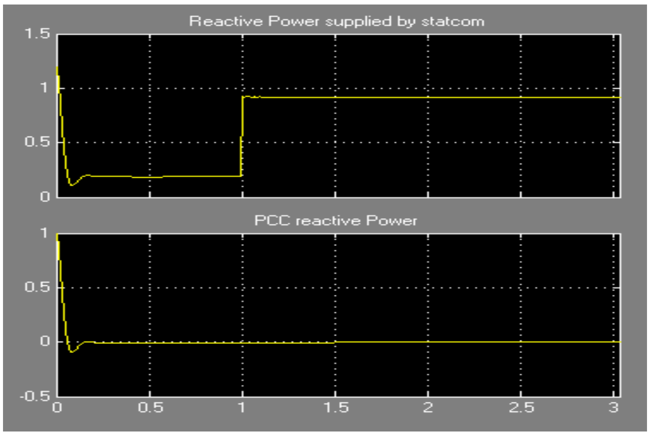

Fig 6.3 STATCOM compensated reactive power.

b. Doubly fed induction generator system with variable speed operation.

In this case, the doubly fed induction generator system variable speed operation is possible by controlling both stator and rotor side. The simulation model for this case is as shown in figure in 6.4.

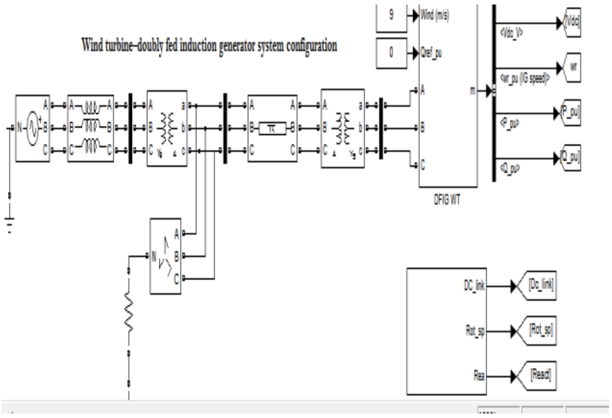

Fig 6.4. doubly fed induction generator system variable speed operation

In doubly fed induction generator system allows the optimal output power operation in the absence of reactive power source. Also the independent control of active and reactive power is achieved.

The steady state results of the doubly fed induction generator system for DC link voltage, rotor speed, active power, reactive power and wind speed as shown in fig 6.5.

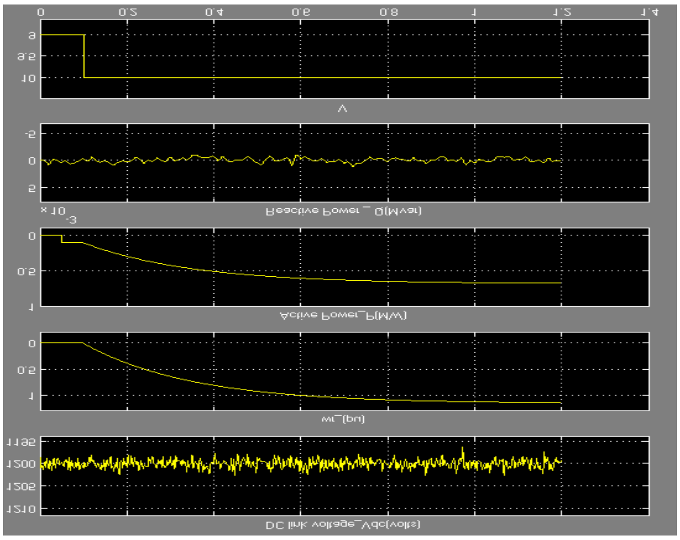

Fig 6.5 DFIG steady state results.

The below waveforms shows that dynamic response to grid voltage droop for the operation of doubly fed induction system.

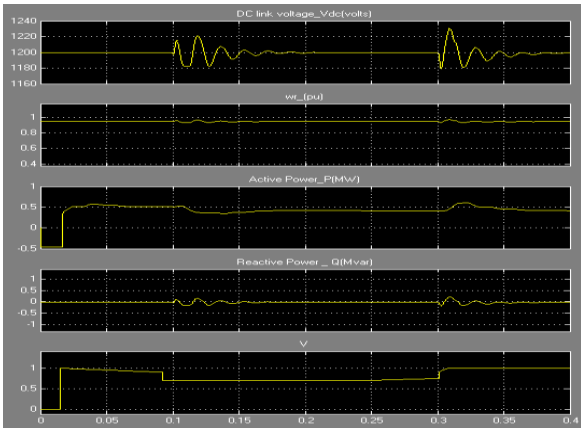

Fig 6.6 Dynamic results for DFIG system.

c) Comparison of the Wind turbine system using SCIG and DFIG systems.

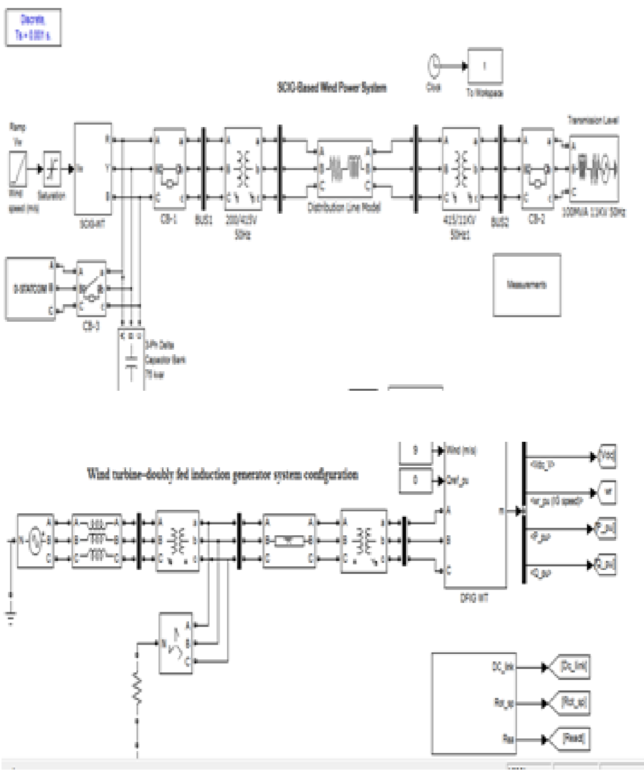

Fig 6.7.Comparison of the Wind turbine system using SCIG and DFIG systems.

The waveform shows that variations between DFIG and SCIG wind power systems using wind turbine operations for the variation in reactive power operation as shown in 6.8.

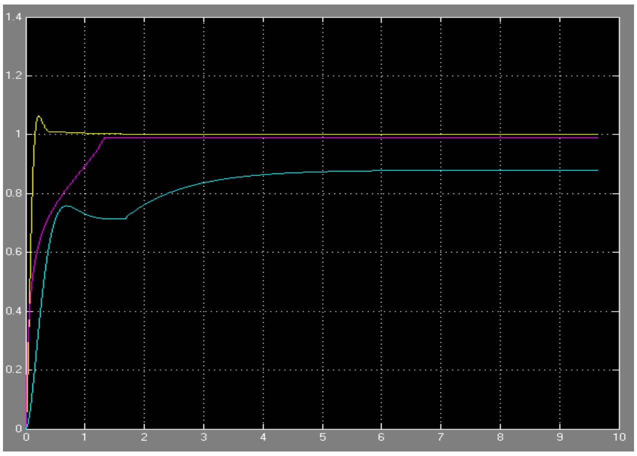

Fig 6.8 Distribution voltage for SCIG and DFIG systems.

CONCLUSION

This project has presented the comparison of the wind turbine systems using SCIG and DFIG generator systems. With the experimentally investigated wind turbine model, a SCIG and a DFIG wind power systems are modeled and simulated in MATLAB/SIMULINK. An optimal active-power-versus-rotor-speed relationship has been proposed for turbine model first, and it functions as a lookup table for tracking the maximum output active power.

The SCIG system presents the need of external reactive power source to support grid voltage, and it can keep the output power at the nominal level by pitch control but cannot accordingly change the rotor speed to achieve maximum wind power capture at different wind speeds. In contrast, the DFIG system does not need reactive power compensator to hold distribution line voltage and achieves optimal active power controlling. Both voltage control schemes for two converters consist of a current regulation part and a cross-coupling part. The turbine emulator system performs well and follows the theoretical and simulated maximum power extraction points in different operating conditions.

The comparison between SCIG and DFIG wind power system using wind power operation can be varied by varying the parameters active power, reactive power, DC link voltage, rotor speed and wind speed can be

ISSN No: 2348-4845
International Journal & Magazine of Engineering, Technology, Management and Research
A Peer Reviewed Open Access International Journal

seen in simulation results by using DFIG wind power system, the system performance can be improved as compare to SCIG wind power system.

REFERENCES

[1] G. Deconinck, "Developing a Distributed Hands-On Course for Teaching Advanced Electrical Engineering Topics", Int. Journal of Electrical Engineering Education (IJEEE) (Manchester University Press), Vol. 44, No.1, Jan. 2007, pp. 1-11.

[2] G. Deconinck, E. Claesen, J. Knockaert, T. Nobels, P. Saey, M. Van Dessel, G. Van Ham, "Guided Self-Study Approach for Advanced Topics in Automation, Control and Electrical Engineering", Proc. of ECUMICT 2010, Ghent, Belgium, March 2010.

[3] M. Van Dessel, G. Deconinck, "Power electronic grid connection of PM synchronous generator for wind turbines", Proc. of the 34th Annual Conference of the IEEE Industrial Electronics Society IECON 2008, 10 – 13 november 2008, pp. 2200-2205.

[4] S. Bequé, J. Dils, M. Van Dessel, "Optimisation of a direct drive low speed permanent magnet wind generator", Proceedings of the Nordic Matlab Conference 2003, Copenhagen, Denmark, 21 – 22 Oct. 2003, pp. 215 - 219.

[5] Fortis Wind Energy Systems, "Wind turbine technical specifications", www.fortiswindenergy.co.uk/index.asp?id=38.

[6] Siemens Automation and Drives Catalogue DA 65/11 "Simovert Masterdrives Motion Control", 'Engineering information' pp. 6/36- 6/65, 2003/2004.

[7] The Mathworks, "Matlab – Simulink SimPowerSystems Users guide", www.mathworks.com.

[8] N. A. Orlando, R. A. Mastromauro, M. Liserre, A. Dell'Aquila, "Grid Voltage Support by Means of a Small Wind Turbine System", Proc. of the IEEE Industrial Electronics Conference IECON 2008, 10 – 13 november 2008, pp. 2178-2183.

[9] S. Li, L. Xu, "PWM Converter Control for Grid Integration of Wind Turbines with Enhanced Power Quality", Proc. of the IEEE Industrial Electronics Conference IECON 2008, 10 – 13 november 2008, pp. 2218-2224.